Enhancing Mechanical Properties of Cement Mortar through Al2O3 Reinforcement

Mohamed Abbas M M[1], Pandikkannu S[1], Killivalavan[1], Kornala Kalyani[1*]
[1]*Department of Civil Engineering, Indian Institute of Industry Interaction Education and Research, Chennai, Tamil Nadu 600066*

***Abstract*—This research investigates the increase of mechanical characteristics of cement mortar with the use of Al_2O_3 reinforcing. Three weight ratios of nanoparticles made of Al_2O_3 with a mean diameter of 15 nm, namely 0.125%, 0.25%, and 0.5% of Al_2O_3 /CNFs, were compared with reference cement mortar specimens without any additives. The weight-to-weight ratios of Al_2O_3/CNFs in cement mortars were evaluated at three levels: 0.5%, 0.25%, and 0.125%. Additionally, the cement mortars without Al_2O_3/CNFs were included as well for comparison with the reference samples. The presence of a reactive and porous layer of alumina facilitated the hydration process and enhanced the formation of a uniformly dispersed hydration gel. The use of Al_2O_3 /CNFs as reinforcement resulted in a higher generation of hydration gel compared to CNFs without reinforcement, as shown by derivative thermal analysis–differential thermogravimetric (TGA-DTG) and X-ray powder diffraction (XRD) characterization. The findings indicate that the most favorable improvement in the characteristics of the cement mortar occurred while using different ratios for CNFs. The addition of Al_2O_3/CNFs significantly improved the compressive strength, reduced the deterioration of compressive strength after 150 cycles, and minimized drying shrinkage in the specimens. The limited utilization of the carbon nanofibers (CNFs) in the Al_2O_3 /CNFs samples suggests that the use of this coating is a cost-effective and encouraging method for enhancing the efficiency of cement mortars.**

***Index Terms*—Al_2O_3 Reinforcement, X-ray powder diffraction, Mortars fabrication and mix propositions.**

I. INTRODUCTION

Cementitious elements have become the most often used building materials. However, they have a poor resistance to being pulled apart and are very prone to developing cracks. Consequently, several research efforts have been focused on improving the cement structure by including reinforcements at either the macro or micro level [1]. Nevertheless, interior holes and fractures often originate as nano-sized embryos and then expand to a micro size, ultimately reaching a threshold of destructiveness. If the majority of voids are located inside the cementitious structure, water may readily infiltrate and cause the precipitation of these voids, potentially resulting in freeze-thaw damage. The structure of cementitious materials is significantly degraded when exposed to repeated freeze-thaw cycles [2]. Hence, the utilization of nano-scale reinforcements serves as an efficient method to safeguard the intrinsic mechanical and durability features by averting the commencement of voids.

In the current era of the construction industry, Portland-cement-based binding compounds are extensively used in the manufacturing of concrete. Additional components used include fine particles, coarse aggregates, and water. The growing use of concrete results in a rise in CO2 emissions, which significantly contributes to global warming and poses health problems associated with pollution. Approximately 1.5 billion metric tons of carbon dioxide (CO2) are released into the environment each year to create ordinary Portland cement (OPC). Furthermore, the CO2 emissions from OPC manufacturing account for approximately 8% of the total global CO2 emissions.

The utilization of supplementary cementitious materials such as silica fume, granulated blast furnace slag, and fly ash has an impact on the carbonation properties of concrete. However, the replacement or substitution of cement with self-compacting concrete significantly improves the fundamental engineering properties of concrete. The presence of crystalline and glassy phases in fly ash and GGBS enhanced the cementitious properties and hydration characteristics of the binding material. The use of fly ash has increased the strength properties of traditional concrete by up to 20% [3]. Furthermore, the increase in the additional amount of binding material with GGBS enhances the shrinkage strain characteristics of the concrete. The impact of Ground Granulated Blast Furnace Slag (GGBS) on Ultra-High-Performance Concrete (UPHC) is quite substantial, and the performance of UPHC is almost equivalent to that of ordinary concrete when GGBS is used as a replacement material at levels up to 40%.

The increase in the global population and the rapid urbanization have led to a conflict between the need for more civil engineering projects and the worsening ecological conditions.

This conflict has, in turn, driven the construction industry to focus on achieving high efficiency, high performance, and sustainability. Conventional concrete utilizes Portland cement as its primary binding element, and its implementation has established a strong basis for the advancement of the contemporary building sector. Nevertheless, the production of each metric ton of Portland cement results in the emission of 0.55-0.95 metric tons of carbon dioxide [4]. As the demand for it grows, the environmental difficulties caused by its manufacturing method are becoming more evident. The pursuit of high-performance and ecologically sustainable green cementitious materials has become imperative in the advancement of concrete technology.

Furthermore, the building sector has two prominent challenges: the excessive use of non-renewable resources and the substantial buildup of construction waste. A substantial depletion of natural sand and gravel reserves is occurring, resulting in a scarcity of these natural resources. Simultaneously, as a result of the city's inherent "metabolism," a substantial quantity of construction debris has accumulated owing to extensive rehabilitation, demolition, and other related operations. As a result, experts have suggested the use of recycled concrete technology to enhance the efficiency of converting building waste into usable resources. This study examines the effects of nano-Al_2O_3 on the flexural and tensile strength, as well as the setting time, of binary mixed concrete. The alumina component undergoes a reaction with the calcium hydroxide that is formed during the hydration process of calcium silicates. The rate of the pozzolanic reaction is directly related to the quantity of accessible surface area for the reaction. Hence, it is feasible to use high-purity nano-Al_2O_3 (99.9%) with a high Blaine fineness value (60 m2/g) to enhance the properties of cement mortars.

Rest of the work is organized as; Section 2 presented the literature survey followed by the materials and methods are explained in Section 3. Section 4 shows the experimental investigation and the paper concluded in Section 5.

II. RELATED WORKS:

Wang et al. [5] conducted a study on improving the durability and mechanical performance of incinerator bottoms made from Al2O3 using a high strength mortar. The ALMP increased the UPV by a range of 3.16% to 9.49%, and the DME by a range of 9.64% to 18.69%. In addition, we saw a significant decrease in drying shrinkage in HSM by 4.96% to 28.36% and a reduction in the chloride migration coefficient by 7.45% to 38.75% as a result of the presence of ALMP. After evaluating the effects of ALMP on HSM's workability, mechanical characteristics, and microstructure, we recommend a doping quantity of 10 wt% as the most suitable for ALMP in HSM. Our analysis suggests that using IBA for typical quartz sand in the manufacturing of HSM might possibly reduce energy usage, carbon emissions, and production costs. The results of this work may have important implications for enhancing the efficient use of IBA in cement-based products.

Li et al. [6] introduced the use of SiO2 and Al2O3 nanoparticle reinforcements in order to enhance the properties of cementitious materials. The findings indicate that the addition of NA and NS to concrete may enhance its compressive strength and resistance to chloride penetration (RCP). The optimal effect is seen with the addition of 1 and 2 wt%, particularly in terms of compressive strength, which can be enhanced by over 20%. NA and NS, which are particles at the nanoscale, have the ability to occupy the small holes in concrete and enhance the process of cement hydration. This results in the production of more C-S-H gel, leading to a decrease in the overall porosity of the concrete by about 2%. Consequently, the internal pores and fractures become smaller, and the microstructure of the concrete becomes more compact. The correlation study revealed the key elements that influence the compressive strength and RCP ability of concrete. Additionally, a linear connection equation between compressive strength and RCP ability was derived.

Ting et al. [7] examined the mechanical characteristics of recycled brick aggregate concrete microstructure, specifically focusing on the impacts of nano-materials reinforced aggregate. The findings indicate that the water absorption of recycled brick aggregate diminishes when the concentration of nanomaterials solution increases, and the crush index of recycled brick aggregate also falls. The addition of nano-SiO2 and nano-Al2O3 enhances the compressive strength of recycled brick aggregate concrete at all stages of its development. Notably, the impact of nanomaterials on the early strength of concrete is more pronounced. The compressive strength of nano-SiO2 reinforced brick aggregate concrete first rises and subsequently falls with the rise in nano-solution concentration. Conversely, the compressive strength of nano-Al2O3 reinforced brick aggregate concrete shows a continuous increase. The nanomaterial-reinforced brick aggregate has a more compact internal structure, with denser arrangement and filling of micro fractures and pores with hydration products. Additionally, the interfacial transition zone is more tightly packed.

Ankamma et al. [8] introduced hybrid nano-composites as a means to study and enhance the strength of traditional cement concrete. The binding material in concrete mixes was substituted with various nanoparticles, namely nano-Fe2O3 and nano-Al2O3, at four different replacement rates (up to 4%). This substitution brings about a certain alteration in the building materials and provides energy to the structure. The slump cone test was conducted to evaluate the workability of concrete mixes. The strength properties of the mixes were assessed, including the compressive, split tensile, and flexural strengths, after 7, 28, and 90 days of hardening. Furthermore, the slump value of the combination fell as the replacement rate of nanoparticles increased. Nevertheless, the slump values remained within the allowed range for workability and did not have any impact on the compaction of the concrete. Nevertheless, the increase in strength of the hybrid nano mixes was comparable to that of the mixtures containing solely nano-Fe2O3 or nano-Al2O3. The test findings demonstrated that nanoparticles have the ability to augment the strength and microstructure characteristics of concrete.

Feng et al. [9] introduced a composite material of reinforced magnesium phosphate cement, using nano-Al2O3 and fiber to enhance its mechanical characteristics. The variables in the experimental examination included the fiber kinds, fiber volume percentage, nano-Al2O3 replacement rate, and curing duration. Adding nano-Al2O3 was shown to enhance both the workability and mechanical characteristics of the MPC, as demonstrated by the experimental findings. The workability exhibited a progressive decline as the fiber content rose, although both the compressive and tensile strength showed a gradual rise. Out of several fiber kinds, the micro-steel fiber (MSF) had the greatest impact on enhancing flexural toughness. The empirical equations for forecasting the compressive strength and splitting tensile strength of fiber and nano-Al2O3 reinforced MPC composite (FNRMC) were developed based on the study of experimental data. Furthermore, XRD and SEM were used to investigate the microscopic phase tests and uncover the modification methods of nano-Al2O3 on the MPC.

III. MATERIALS AND METHODS

The mortar mix was prepared using Ordinary Portland cement, which falls within the ASTM C150 standard type I classification. All mixes used natural river sand with a fineness modulus of 2.6. In order to improve the workability, a water-reducing admixture was used. Carbon nanofibers (CNFs) with a diameter ranging from 50 to 150 nm were used in this investigation. The precursor utilized for coating was trimethylaluminum (TMA-1.0M). Table 1 displays the physical and chemical parameters of Portland cement.

A) Aggregates

The fine aggregate utilized was locally sourced natural sand, which had fragments less than 0.5mm, a modulus of fineness of 2.25, and a 2.58g/cm3 of specific gravity. The coarse aggregate used in the laboratory was crushed basalt with a maximum size of 15mm and specific gravity of 2.96g/cm³ [10].

B) CNFs coating based on Al_2O_3 synthesis

The deposition of Al_2O_3 coating on CNFs was achieved by the use of a condensed layer deposition (CLD) technique. The carbon nanofibers (CNFs) underwent surface treatment using a combination of sulfuric acid and nitric acid. The volume ratio of the acids was 3:1, with a concentration of 6.0 M. The treatment was carried out under a sonication probe for

2 hours at a temperature of 60°C. Subsequently, the CNFs were washed with deionized water to eliminate any remaining acid residue [11]. The coating procedure was conducted in separate batches, with each batch consisting of 400 mg of CNF dispersed in 500 mL of heptane. This dispersion was divided equally into two containers, with each container containing 200 mg of CNFs in 250 mL of heptane. Following a 20-minute period of sonication, 150 microliters of water were introduced into the mixture while simultaneously subjecting it to sonication and stirring. After a further 20 minutes, a thin layer of water developed on the surface of the CNFs. Next, a quantity of 0.00789 moles of TMA was introduced into the reaction mixture. This was done beneath a nitrogen blanket to ensure that the presence of the atmosphere would not have any impact on the reaction. The reaction itself is represented by the equation $2TMA + 3H_2O \rightarrow Al_2O3 + 6CH_4$. The specimens were dehydrated using a vacuum at a temperature of 100°C for a duration of 8 hours. A further annealing process was carried out at a temperature of 350°C for a duration of 2 hours in a tube furnace, with the purpose of eliminating any remaining CHx residues

C) Mortars fabrication

The cement-to-sand ratio was maintained at a constant 1:2, while the water-to-cement ratio was set at 0.35. Three distinct ratios of cellulose nanofibers (CNFs) and aluminum oxide (Al_2O_3)/CNFs, with weights of 0.125%, 0.25%, and 0.5%, were formulated [12]. Furthermore, a control sample without nanomaterial, referred to as C0, was created and the blending characteristics are shown in Table 2. As part of a standard process, suspensions of CNFs and Al_2O_3/CNFs may be created by subjecting them to sonication (at 800 W–20 kHz) in water while simultaneously swirling mechanically for a duration of 30 minutes. Subsequently, this water may be used as a blending ingredient for the preparation of composite mortars. In order to enhance the smoothness of the mixture, a certain proportion of a superplasticizer was introduced either to the combination of water and nanomaterials or only to water. The superplasticizer, functioning as a surfactant, was only used in the solutions containing just CNFs. For the Al_2O_3/CNFs, 80% of water was used to disperse the Al_2O_3/CNFs, while the remaining 20% was combined with superplasticizer. Figure 1 depicts the blending techniques used for the Al_2O_3/CNFs composites. Subsequently, the newly prepared mixture was poured into several molds to facilitate the distinct testing methods outlined in this document.

Table 1: Portland cement chemical properties (Wt. %)

Materials	**Cement**
SiO_2	21.89
AL_2O_3	5.3
Fe_2O_3	3.34
CaO	53.27
MgO	6.45

D) Characterization models

Characterizations of surface

Two methods of surface evaluation were used. The Al_2O_3 coating on CNFs was assessed using Transmission Electron Microscopy (TEM) using a Jeol-1400 instrument operating at an acceleration voltage of 120 kV. The cement internal structure was examined using an FEI Quanta 600 FEG scanning electron microscopy (SEM) instrument [13]. The scanning electron microscope (SEM) was configured with a voltage of 5 kV to enhance sensitivity in capturing surface structures. The surface area of both Al_2O_3/CNFs and the cement composites was determined using the Brunauer–Emmett–Teller technique.

X-ray Diffraction Analysis

An XRD (X-ray diffraction) study was conducted using a Philips X-Pert-Fisher Scientific instrument in Hampton, NH, USA. The instrument was outfitted with CuKα to determine the crystal structure of the materials. Data was gathered within the angle that ranged from $2\theta = 5°–90°$, with a scan rate of 0.026° s^{-1}. The materials, weighing 50 mg, were fragmented and separated using a 75 µm sieve.

Tests of drying shrinkage

The shrinkage during drying experiments were conducted on cement mortar samples with a water-to-cement ratio (w/c ratio) of 0.4. The samples had dimensions of 25 mm × 25 mm × 280 mm, and measurements were carried out following the guidelines outlined in ASTM C596. The samples were removed from the molds 48 hours after being cast and then immersed in lime water [14]. After a period of 72 hours had elapsed from casting, the samples were taken out of the lime water and the original dial gauge measurement of their length was recorded. The length measurements were performed using a length comparator in accordance with the ASTM C490/C490M-17 standard. The biological samples were kept in a dehumidified chamber at a temperature of 22 ± 4 °C and with a relative moisture of 90%. The length change measures were recorded at the ages of 5, 7, 14, 28, and 56 days.

Tests of Freeze–Thaw

In order to assess the resilience of both the untreated and reinforced mortars, a freeze-thaw cycling procedure was carried out according to ASTMC666 guidelines. This included subjecting the samples to a temperature range of -18 °C to 4 °C, with fast freeze-thaw cycling taking place in water. The specimens were rectangular prisms with dimensions of 25 mm × 25 mm × 280 mm. Prior to the freeze-thaw test, the specimens were removed from the molds and subjected to a 28-day period of moist-curing. The samples underwent a minimum of 300 freeze-thaw cycles. The decrease in mass of all composite mortars and the decline in compressive strength of composites with the most effective amount of nanomaterials were quantified after a predetermined number of freeze-thaw cycles.

IV. EXPERIMENTS

Figure 1(i) illustrates the dispersion of untreated CNFs and Al2O3/CNFs in water, both before and after surface functionalization. Additionally, Figure 1(i) shows the dispersion of Al2O3/CNFs before and after annealing at 350 °C in the presence of air. The observations were conducted after a 30-minute sonication procedure without the inclusion of any surfactant, and the various solutions were allowed to sit for a duration of 30 days. The untreated CNF solution exhibited no dispersion, but the treated CNFs solution had reasonably favorable dispersion. However, after a period of 30 days, several CNF clusters were clearly observable in the lowermost part of the vials. The Al2O3/CNFs precipitated in water as a result of the residual organic ligands from the coating precursor molecule. The situation underwent a significant change after the exposure of the newly prepared Al2O3/CNFs to air at a temperature of 350 °C for one hour. Consequently, the suspensions of annealed Al2O3/CNFs exhibited much superior long-term stability in comparison to other suspensions. The elimination of organic residues was verified using TGA analysis, as seen in Figure 1 (ii). The improved dispersion may be related to the creation of pores resulting from the oxidation of the organic material, which transforms them into surfaces that are very hydrophilic.

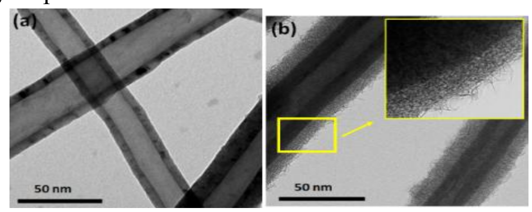

Figure 1: TEM Bright-field results

The physical appetites of the samples after 300 cycles are shown in Figure 2. The improvement may be attributed to the responsiveness of the permeable Al_2O_3 layer, which expedites the process of hydration, resulting in the formation of more evenly distributed C-S-H hydrated gels inside the structure. The presence of a reduced number of CH crystals and an increased amount of amorphous C-S-H in Al_2O_3 /CNFs-0.125%, as seen by SEM, XRD, and TGA/DTA, provides evidence supporting this hypothesis. The presence of tiny spaces may reduce the time it takes for water to settle and slow down the increase in ice volume. This outcome is anticipated due to the presence of a vacuum with tiny dimensions, which would result in a significant internal pressure and surface tension in accordance with the rules of physics. The use of well-dispersed nanomaterials into the mortar matrix significantly improved its frost resistance. Al_2O_3/CNFs composites exhibited a notable resilience to frost.

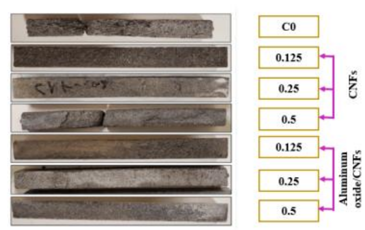

Figure 2: Samples physical appetences after the cycles of 300

Figure 3 displays the assessment of split tensile strength (measured in MPa). The split tensile strength data for mixes in series C0 and N are shown in Table 4. The comparison of the data obtained from the samples taken at 7, 28, and 90 days reveals that the split tensile strength exhibits an increase when nano-Al_2O_3 particles are added up to a replacement level of 1.0%. However, beyond this level, the split tensile strength starts to drop. It is worth noting that even at a replacement level of 2.0% (N4), the split tensile strength remains greater than that of the plain cement concrete (C0). The use of 2.0% particles has been shown to reduce the split tensile strength to a level that is comparable to the control concrete. This could be attributed to an excessive amount of particles in the mixture, surpassing the necessary quantity for reacting with the released lime during hydration. Consequently, an excess of silica is leached out, resulting in a deficiency in strength. This occurs because the silica replaces a portion of the cementitious material but does not contribute to the overall strength. Additionally, weak zones may arise as a result of faults occurring during the dispersion of nanoparticles.

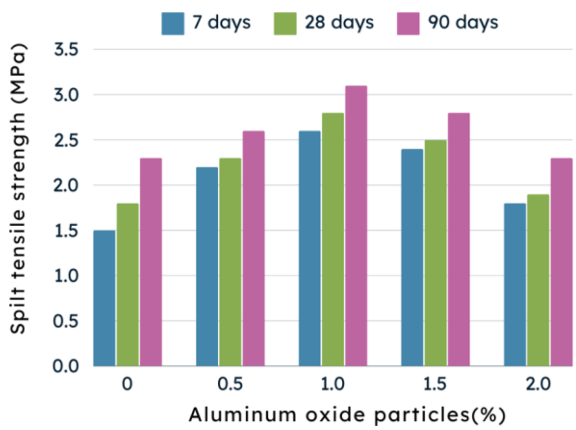

Figure 3: Performance evaluation for split tensile strength (MPa)

The mass loss performance is displayed in Table 3. The weight fluctuations were observed during the freeze-thaw cycles, which were performed after 50, 100, 150, 200, 250, and 300 cycles. Table 3 demonstrates that the mass loss of all mixes escalated as the number of freeze-thaw cycles increased. The incorporation of nanoparticles resulted in a substantial decrease in the mass loss seen in the samples. For the control sample C0, the average mass loss was around 9% after 300 cycles. However, when CNFs were added at various ratios, the mass loss consistently decreased. The lowest mass loss was found in the case of CNFs-0.25%. This suggests that the incorporation of the functionalized carbon nanofibers (CNFs) successfully decreased the amount of empty space and enhanced the compactness of the CNF/cement composites. Nevertheless, the rate of mass loss escalated when CNFs-0.5% was included into cement mortars. This outcome was anticipated as these composites exhibited reduced strength as a result of the formation of large holes in the matrix owing to the clustering of the CNFs bundles.

Table 3: Mass loss performance

Number of cycles	Mass loss (%)						
	C0	CNF-0.125%	CNF-0.25%	CNF-0.5%	Al_2O_3/CNF-0.125%	Al_2O_3/CNF-0.25%	Al_2O_3/CNF-0.5%
50 cycles	0.3	0.4	0.2	0.5	0.2	0.1	0.2
100 cycles	0.7	0.5	0.3	0.4	0.6	0.2	0.3
150 cycles	1.3	1.5	1.0	1.1	1.4	1.6	1.3
200 cycles	1.6	1.8	1.3	1.9	1.4	1.3	1.2
250 cycles	2.5	2	1.9	1.8	1.5	1.6	1.4
300 cycles	8.5	2.6	1.9	6.5	1.2	2.7	1.7

The performance evaluation for flexural strength is displayed in Figure 4. The flexural strength of the specimens follows a similar trend to the tensile strength, increasing with the addition of nano-Al2O3 particles up to a 1.0% replacement (N2). However, beyond this point, the flexural strength drops. It is worth noting that even at a 2.0% replacement (N4), the flexural strength is still greater than that of ordinary cement concrete (C0). The increase in flexural strength is attributed to the quick consumption of Ca(OH)2, which is generated during the hydration of Portland cement, particularly during the early stages owing to the strong reactivity of nano-Al2O3 particles.

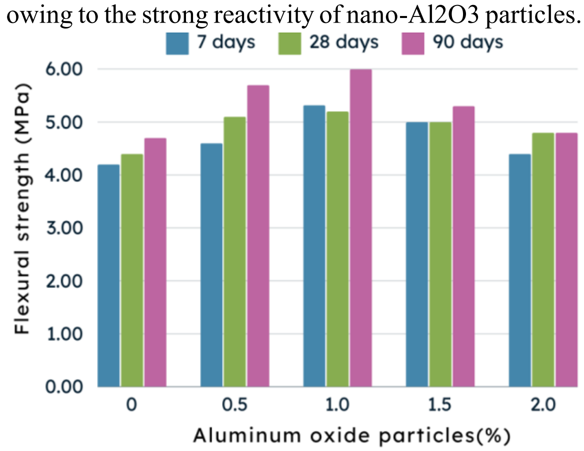

Figure 4: Performance evaluation for flexural strength (MPa)

The performance evaluation for compressive strength is outlined in Figure 5. The compressive strength of the specimens exhibits a similar pattern to the tensile strength, escalating as the nano-Al2O3 particles are included, reaching a peak at a 1.0% substitution (N2). However, after reaching this stage, the flexural strength decreases. It is important to mention that even with a 2.0% replacement (N4), the flexural strength remains higher than that of conventional cement concrete (C0). The rise in flexural strength is ascribed to the rapid use of Ca(OH)2, which is produced during the hydration of Portland cement, especially in the first phases due to the high reactivity of nano- particles of Al2O3.

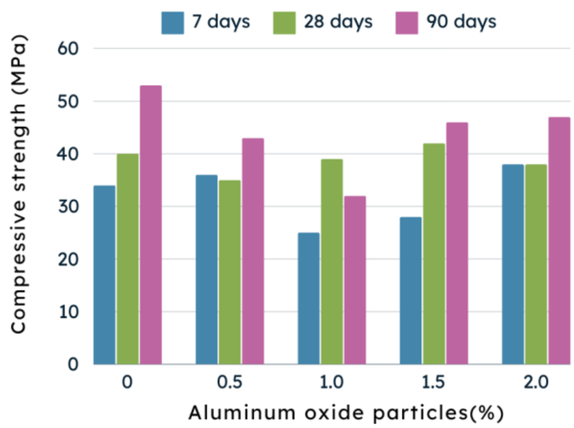

Figure 5: Performance evaluation for compressive strength (MPa)

The performance analysis of pore diameter is displayed in Table 4. The cement mortar powder underwent granulation and filtration using a 300 µm screen. Subsequently, it was subjected to drying and vacuuming at a temperature of 200 °C for a duration of 2 hours as part of the degassing process. The pore volume of the samples was determined. The total BJH pore volume was determined to be 0.07805, 0.06783, and 0.06278 mL/g for C0, CNFs-0.25%, and Al2O3/CNFs-0.125%, respectively. The data displays the statistical measurements of pore size for the three samples. The pore diameter statistic is categorized into four distinct sections. The Al2O3/CNFs-0.125% exhibited holes with a larger volume ranging from 1 to 10 nm, which are categorized as gel pores. The gel holes are associated with the generation of calcium-silicate-hydrate (C-S-H), which is often formed by the hydration reaction of tricalcium silicate (C3S) and dicalcium silicate (C2S). In different ranges, where capillary pores exist, the pore volume of Al2O3/CNFs-0.125% was noticeably decreased, suggesting an improvement in refining. Incorporating CNFs also resulted in pore refinement. However, the addition of Al2O3/CNFs-0.125% further decreased the pore volume. This might be attributed to the greater C-S-H concentration, as shown by the TGA and XRD data. The presence of the Al2O3 nanocoating may contribute to the occurrence of the pozzolanic reaction, resulting in the formation of additional C-A-H.

Table 4: Performance analysis of pore diameter in nm

Pore diameter (nm)	Pore volume		
	C0	CNFs-0.25%	Al_2O_3/CNFs-0.125%
1-10	0.018	0.02	0.023
10-20	0.014	0.01	0.01
20-80	0.040	0.026	0.02
>80	0.010	0.008	0.007

V. CONCLUSION

This research examined the impact of incorporating Al2O3/CNFs on the strength under compression, freeze-thaw durability, and drying shrinkage of cement mortars. Despite the findings demonstrating the feasibility of the technique, the research was subject to several limitations. Currently, the stability of the Al2O3 nanolayer at high concentrations of the superplasticizer, which is an acidic chemical, remains uncertain. Furthermore, this work does not include an analysis of the impact of alumina-coated carbon nanofibers on drying shrinkage under varied water-to-cement ratios and varying temperatures. The extent to which the integration of Al2O3/CNFs has refined the pores has not been quantified using a direct approach such as water absorption or mercury intrusion porosimeter. Research has shown that the cement may be effectively substituted with nano-Al2O3 elements, up to a maximum threshold of 2.0%, with a mean size of the particles of 15 nm.

VI. REFERENCES

[1] Nivethitha, D., Srividhya, S. and Dharmar, S., 2016. Review on mechanical properties of cement mortar enhanced with nanoparticles. International Journal of Science and Research (IJSR), 5(1), pp.913-6.

[2] Win, T.T., Prasittisopin, L., Jongvivatsakul, P. and Likitlersuang, S., 2023. Investigating the synergistic effect of graphene nanoplatelets and fly ash on the mechanical properties and microstructure of calcium aluminate cement composites. Journal of Building Engineering, 78, p.107710.

[3] Chu, H., Wang, Q. and Zhang, W., 2024. Optimizing ecological ultra-high performance concrete prepared with incineration bottom ash: Utilization of Al2O3 micro powder for improved mechanical properties and durability. Construction and Building Materials, 426, p.136152.

[4] Humad, A.M., Dakhil, A.J., Al-Mashhadi, S.A., Al-Khafaji, Z., Mohammed, Z.A. and Jabr, S.F., 2023. Improvements of mechanical and physical features of cement mortar by nano **AL2O3** and **CaCO3** as additives.
[5] Wang, Q., Chu, H., Jiang, J. and Zhu, B., 2024. Enhancing mechanical performance and durability of high strength mortar with incineration bottom ash via Al2O3 micro-powder: An experimental study. Journal of Building Engineering, p.109268.
[6] Li, C., Cao, Y., Li, G., Liang, Q., Wu, X., Wu, G., Wang, F., Du, Q., Wang, Y., Qi, S. and Tang, L., 2023. Modified cementitious materials incorporating Al2O3 and SiO2 nanoparticle reinforcements: An experimental investigation. Case Studies in Construction Materials, 19, p.e02542.
[7] Ting, W.A.N.G., Qingshan, W.A.N.G., Shenao, C.U.I., Haihe, Y.I., Tian, S.U. and Zhenyu, T.A.N., 2023. Effects of nanomaterials reinforced aggregate on mechanical properties and microstructure of recycled brick aggregate concrete. Materials Science, 29(3), pp.347-355.
[8] Ankamma, V. and Kumar, A.S., 2023. Investigation study of enhance the strength by using hybrid nano-composites on conventional cement concrete. Materials Today: Proceedings, 72, pp.2939-2945.
[9] Feng, H., Shen, S., Pang, Y., Gao, D., Wang, Z. and Sheikh, M.N., 2021. Mechanical properties of fiber and nano-Al2O3 reinforced magnesium phosphate cement composite. Construction and Building Materials, 270, p.121861.
[10] Meddah, M.S., Praveenkumar, T.R., Vijayalakshmi, M.M., Manigandan, S. and Arunachalam, R., 2020. Mechanical and microstructural characterization of rice husk ash and Al2O3 nanoparticles modified cement concrete. Construction and Building Materials, 255, p.119358.
[11] Qader, A. and Noori, H.J., 2021. Enhancing the mechanica and durability properties of cement mortars by using alumina nanocoating on carbon nanofibers (Doctoral dissertation, University of Missouri--Columbia).
[12] Feng, H., Zhu, P., Guo, A., Cheng, Z., Zhao, X. and Gao, D., 2022. Assessment of the mechanical properties and water stability of nano-Al2O3 modified high ductility magnesium potassium phosphate cement-based composites. Materials Today Communications, 30, p.103179.
[13] Orakzai, M.A., 2021. Hybrid effect of nano-alumina and nano-titanium dioxide on Mechanical properties of concrete. Case Studies in Construction Materials, 14, p.e00483.
[14] Seifan, M., Mendoza, S. and Berenjian, A., 2021. A comparative study on the influence of nano and micro particles on the workability and mechanical properties of mortar supplemented with fly ash. Buildings, 11(2), p.60.